Particle acceleration during magnetic reconnection in a low-beta pair plasma

Fan Guo, Hui Li, William Daughton, Xiaocan Li, and Yi-Hsin Liu

View Online   Export Citation   CrossMark

ARTICLES YOU MAY BE INTERESTED IN

Particle acceleration during magnetic reconnection in a low-beta pair plasma

Fan Guo,[1,a)] Hui Li,[1] William Daughton,[1] Xiaocan Li,[2] and Yi-Hsin Liu[3]
[1]*Los Alamos National Laboratory, Los Alamos, New Mexico 87545, USA*
[2]*Department of Space Sciences, University of Alabama in Huntsville, Huntsville, Alabama 35899, USA*
[3]*NASA Goddard Space Flight Center, Greenbelt, Maryland 20771, USA*

Plasma energization through magnetic reconnection in the magnetically dominated regime featured by low plasma beta ($\beta = 8\pi nkT_0/B^2 \ll 1$) and/or high magnetization ($\sigma = B^2/(4\pi nmc^2) \gg 1$) is important in a series of astrophysical systems such as solar flares, pulsar wind nebula, and relativistic jets from black holes. In this paper, we review the recent progress on kinetic simulations of this process and further discuss plasma dynamics and particle acceleration in a low-β reconnection layer that consists of electron–positron pairs. We also examine the effect of different initial thermal temperatures on the resulting particle energy spectra. While earlier papers have concluded that the spectral index is smaller for higher σ, our simulations show that the spectral index approaches $p = 1$ for sufficiently low plasma β, even if $\sigma \sim 1$. Since this predicted spectral index in the idealized limit is harder than most observations, it is important to consider effects that can lead to a softer spectrum such as open boundary simulations. We also remark that the effects of three-dimensional reconnection physics and turbulence on reconnection need to be addressed in the future. *Published by AIP Publishing.* [http://dx.doi.org/10.1063/1.4948284]

I. INTRODUCTION

Magnetic reconnection breaks and rejoins magnetic field lines of force, and reorders magnetic topology. Through this process, the magnetic energy is converted into plasma kinetic energy in bulk plasma flow, thermal, and nonthermal particle distributions.[1,2] Reconnection plays a significant role in a wide range of laboratory, space, and astrophysical systems.[3,4] An important problem that remains unsolved is the acceleration of nonthermal charged particles in the reconnection region. While observations have shown strong evidence of particle acceleration associated with magnetic reconnection,[5–7] the primary acceleration mechanism is still under debate.[8–21] It is worthwhile to point out that the acceleration mechanism may depend critically on how reconnection actually proceeds in large 3D system, a subject which is currently an active area of research. During the past decade, it has been shown by both two-dimensional magnetohydrodynamic (MHD) simulations and particle-in-cell (PIC) kinetic simulations that for a large system with weak collisions, the secondary tearing instability leads to fractal reconnection layers with chains of plasmoids developed and the reconnection rate can be independent of the Lundquist number.[22–25] However, effects such as MHD turbulence and 3D physics that could be important to the physics of magnetic reconnection have not been fully understood to reach a consensus.[19,26–32]

In astrophysical problems, such as solar flares, pulsar wind nebula, and relativistic jets in gamma-ray bursts and active galactic nuclei, magnetic reconnection is often invoked to explain high-energy emissions from the strongly magnetized flows.[33–42] For relativistic plasmas, it is useful to define the magnetization parameter $\sigma \equiv B^2/(4\pi nmc^2)$, which indicates the ratio of the energy density of the magnetic field to the rest energy density of the plasma. For nonrelativistic plasmas, it is more appropriate to use plasma beta $\beta = 8\pi nkT/B^2$ that represents the ratio between plasma thermal energy and magnetic energy. In high-energy astrophysics, it is often estimated that the magnetization parameter can be much greater than unity $\sigma \gg 1$ (or $\beta \ll 1$), and the Alfvén speed approaches the speed of light $v_A \sim c$. To explain the observed high-energy emissions, often an efficient mechanism from energies in the magnetized flow into nonthermal particles is required [e.g., Refs. 37 and 43]. In the high-σ regime, magnetic reconnection is the major candidate for converting magnetic energy and producing nonthermal particles and radiations. For a number of other systems such as solar corona and disk corona,[44,45] although the Alfvén speed is not relativistic, the magnetic energy can greatly exceed the plasma thermal energy, so $\beta \ll 1$. During magnetic reconnection, a large fraction of the magnetic energy can be unleashed explosively into plasmas within a short time typically on the order of the Alfvén crossing time.

Much of the recent progress on particle energization during reconnection has been made through first-principles kinetic simulations that self-consistently include the particle dynamics and the microphysics that is necessary to describe collisionless magnetic reconnection. While earlier numerical studies have identified multiple acceleration processes,[9,11–14,17] recent simulations have revealed an efficient nonthermal acceleration that gives hard power-law like energy distributions.[16,18,19,46–49] In this paper, we summarize the relevant progress in this area. We also further study and clarify particle energization in the magnetically dominated plasmas with focuses on the regime with a low-β pair plasma ($\beta \ll 1$, $m_i = m_e$). We report new results on the influence of the initial plasma temperature on the hardness of the

spectrum. While earlier papers conclude that the spectral index is smaller for higher σ, our simulations show that the spectral index approaches $p = 1$ for sufficiently low plasma β, even if $\sigma \sim 1$. The spectrum is harder than most of the observed energy spectra. This suggests that to explain the observed spectral index, it is important to consider effects that can lead to a softer spectrum such as the effect of open boundaries. We discuss recent progress in Section II. The detailed numerical methods and parameters are presented in Section III. Section IV discusses the main results of the paper. In Section V, we summarize the results and outline several important problems to be addressed in the future.

II. NONTHERMAL PARTICLE ACCELERATION IN MAGNETIC RECONNECTION LAYERS REVEALED BY KINETIC SIMULATIONS

Earlier kinetic studies have identified numerous different acceleration mechanisms in the reconnection layer. Hoshino *et al.*[9] showed that several processes can occur in a single reconnection layer—in the X-line region[50,51] and along the separatrix region,[52,53] particles can get accelerated in the nonideal electric field and then further accelerated due to grad-B drift and the curvature drift in the magnetic pileup region,[54] where the electric field is mostly ideal $\mathbf{E} = -\mathbf{v} \times \mathbf{B}/c$. Drake *et al.*[11] have further developed the Fermi mechanism inside the magnetic islands as particles get bounced at two ends of islands repeatedly.[12] Oka *et al.*[14] summarized a number of basic acceleration mechanisms and concluded that island coalescence region is an important acceleration site. In these regions, the reconnected flux ropes interact and create new reconnection sites. For a large-scale reconnection layer that contains multiple X-points, the acceleration is more complicated and needs to be studied in a collective manner. Dahlin *et al.*,[17] Guo *et al.*,[18] and Li *et al.*[47] have shown that for a large-scale kinetic simulations that contain multiple X-regions, statistically, the curvature drift acceleration along the reconnecting electric field is the dominant acceleration when the guide field is weak. The nonideal electric field only contributes to a small fraction of energy conversion in the simulation. The effect of a guide field that is normal to the reconnection plane can significantly alter the dominant acceleration mechanism.[12,13,51] It should be noted that *in situ* observations at the magnetotail have found evidence for those acceleration mechanisms. Although energetic particles associated with diffusion regions have been discovered and detected by spacecraft observation,[55] the flux ropes appear to be a stronger sources of energetic electrons.[56–58] Betatron acceleration and Fermi acceleration are found to be important acceleration mechanism further away from the X-points.[9,59–62]

Initial kinetic simulations of relativistic magnetic reconnection have found that strongly nonthermal distributions can be generated at the X-line region through direct acceleration in the diffusion region.[63] While particles get further accelerated in the magnetic pileup regions, the overall energy distribution in the whole domain does not show obvious power-law distributions.[64–66] Over the past few years, several groups have reported hard power-law

distributions $1 \leq p \leq 2$ when $\sigma \gg 1$.[16,18,19,46,48,49] These new simulations found power-law distributions in the whole reconnection region, suggesting that reconnection in magnetically dominated regime may be a strong source of nonthermally energetic charged particles. While these results appear to be repeatedly confirmed, the dominant acceleration mechanism and the formation mechanism for the power-law distribution are still under debate. Through tracing the guiding-center drift motions of particles in PIC simulations, Guo *et al.*[18,19] have shown that the dominant acceleration mechanism is a first-order Fermi mechanism through curvature drift motions of particles in the electric field induced by the reconnection generated flows. By considering an energy continuity equation, it has been shown that a power-law distribution can be generated when a continuous injection and Fermi acceleration $dE/dt = \alpha E$ are considered. The solution also gives a general condition for the formation of the power-law particle energy distribution, i.e., the acceleration time scale is shorter than the time scale for particles injected into the reconnection region $\tau_{acc} < \tau_{inj}$. This mechanism gives rise to the formation of hard power-law spectra $f \propto (\gamma - 1)^{-p}$ with spectral index approaching $p = 1$ for a sufficiently high σ and a large system size. Following this work, the power-law distribution has also been reported in nonrelativistic reconnection simulation with a low-β proton-electron plasma,[47] indicating the power-law distribution can develop in a larger parameter regime than previous expected high-σ regime. In the simulations with magnetically dominated proton-electron plasmas, both electrons and protons develop significant power-law distributions.[49] On the other hand, Sironi and Spitkovsky[16] argued that the initial nonthermal energization at the X-line regions is crucial for the generation of the power-law distribution.[63,65] In the vicinity of the X-lines, the initial distribution is energized into a nonthermal distribution even flatter than the overall distribution but with a limited energy range. This nonthermal distribution gets further accelerated in flux ropes to eventually develop into the observed spectra.[67] Nalewajko *et al.*[68] have shown statistically that the acceleration in the island merging region is a dominant source of nonthermal acceleration. However, the analysis is mostly based on the acceleration site rather than the acceleration mechanism.

III. NUMERICAL METHODS

Kinetic studies of magnetic reconnection have shown that current layers with thicknesses on the order of kinetic scales—skin depth d_i or thermal gyroradius ρ_t—are subject to reconnection. We assume a situation where intense current sheets develop within a magnetically dominated plasma. This can be achieved through various processes such as striped wind geometry,[39,69] field-line foot-point motion,[70,71] and turbulence cascade.[72,73] During reconnection, the critical parameters that quantify the energization in the current layer are the magnetization parameter $\sigma_e \equiv B^2/(4\pi n_e m_e c^2)$ and plasma beta $\beta_e \equiv 8\pi n_e k T_e/B^2$. The numerical simulations presented in this paper are initialized from a force-free current layer with $\mathbf{B} = B_0 \tanh(z/\lambda)\hat{x} + B_0 \operatorname{sech}(z/\lambda)\hat{y}$,[18,19,47,74–76] corresponding to a magnetic field with magnitude B_0 rotating by

$180°$ across the central layer with a half-thickness of λ. The initial distributions are Maxwellian with a spatially uniform density n_0 and thermal temperature $T_e = T_i$. Particles in the central sheet have a net drift $\mathbf{U}_i = -\mathbf{U}_e$ to represent a current density $\mathbf{J} = en_0(\mathbf{U}_i - \mathbf{U}_e)$ that is consistent with $\nabla \times \mathbf{B} = 4\pi \mathbf{J}/c$. Since the force-free current sheet does not require a hot plasma component to balance the Lorentz force, this initial setup may be more suitable to study reconnection in low β and/or high-σ plasmas. We have also used relativistic Harris current sheet[64,77] and found that the two initial setup generally gives similar results, although the hot plasma component in general results in a Maxwellian-like distribution that may dominate over the nonthermal distribution.

In our present simulations, we assume plasma consists of electron–positron pairs with mass ratio $m_i/m_e = 1$. No external guide field is included but there is an intrinsic guide field associated with the central sheet for the force-free setup. During the evolution, the guide field will be expelled from the layer into the flux rope/island regions, and later, the current sheet closely resembles antiparallel reconnection.[75] In this study, we vary the initial thermal temperature to examine its influence on the resulting energy spectra. This has not been fully examined in previous papers. The full particle simulations are performed using the VPIC code,[78] which explicitly solve Maxwell equations and push particles in a relativistic manner. In the simulations, σ is adjusted by changing the ratio of the electron gyrofrequency $\Omega_{ce} = eB/(m_ec)$ to the electron plasma frequency $\omega_{pe} = \sqrt{4\pi ne^2/m_e}$, $\sigma \equiv B^2/(4\pi n_e m_e c^2) = (\Omega_{ce}/\omega_{pe})^2$. We primarily focus on 2D simulations with $\sigma = 1 \rightarrow 100$ and box sizes $L_x \times L_z = 300d_i \times 150d_i$, $600d_i \times 300d_i$, and $1200d_i \times 600d_i$, where d_i is the inertial length c/ω_{pe}. We also show a 3D simulation that discussed previously.[18,19] The 3D simulation has dimensions $L_x \times L_y \times L_z = 300d_i \times 194d_i \times 300d_i$ ($N_x \times N_y \times N_z = 2048 \times 2048 \times 2048$), $kT_e = kT_i = 0.36m_ec^2$, and $\sigma = 100$. The half-thickness of the current sheet is $\lambda = 6d_i$ for all cases. For both 2D and 3D simulations, we have averagely more than 100 electron–positron pairs in each cell. The boundary conditions for 2D simulations are periodic for both fields and particles in the x-direction, while in the z-direction, the boundaries are

conducting for the field and reflecting for the particles. In the 3D simulations, the boundary conditions are periodic for both fields and particles in the y-direction, while the boundary conditions in the x- and z-directions are the same as the 2D cases. A weak long-wavelength perturbation[79] with $B_z = 0.03B_0$ is included to initiate reconnection. All the simulations presented here show excellent energy conservation with violation of energy conservation small enough to accurately determine the particle energy spectra [see the related discussion in Ref. 19].

IV. SIMULATION RESULTS

Figure 1 shows the evolution of the current layer for force-free setup in two-dimensional simulations with $\sigma = 100$. For comparison, a 2D cut from a three-dimensional simulation from earlier studies[18,19] is also presented. They show some common features for such 2D and 3D kinetic simulations of magnetic reconnection starting from a perturbation. For the 2D case, the current sheet first thins down under the influence of the perturbation. The extended thin sheet then breaks into many fast-moving secondary plasmoids due to the growth of the secondary tearing instability. These plasmoids coalesce with each other and eventually merge into a single island on the order of the system size. In the pair plasma case, it has been shown that this secondary tearing instability and plasmoids facilitate fast reconnection and energy release.[18,19,80] The 3D simulations show that the kink instability develops and interacts with the tearing mode, leading to a turbulent reconnection layer.[18,19,81] It has been shown that although the strong 3D effects can modify the current layer, small-scale flux-rope-like structures with intense current density develop repeatedly as a result of the secondary tearing instability.[19] The reconnection rate is roughly the same for the two cases.[19]

The evolution of the reconnection layer in the 3D simulation is shown in Figure 2, which shows several snapshots of volume rendering of the current magnitude. Similar to the 2D case, initially, the layer thins down under the perturbation that is uniform in the y-direction. However, the tearing instability and kink instability rapidly grow and the reconnection layer becomes strongly turbulent. Throughout the simulation,
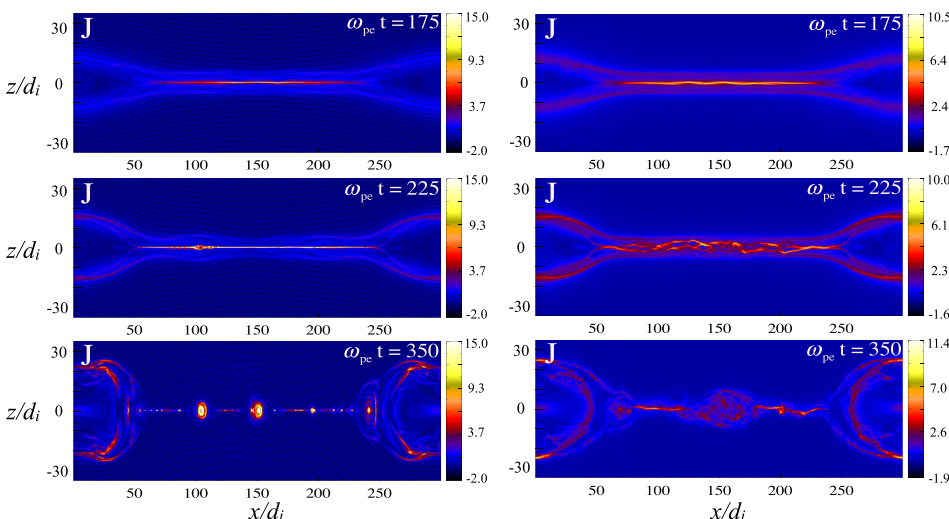

FIG. 1. Time evolution of 2D and 3D simulations with $\sigma = 100$. Left: Color-coded current density at $\omega_{pe}t = 175$, 225, and 350, respectively. Right: 2D cut of current density from the 3D simulation at $\omega_{pe}t = 175$, 225, and 350, respectively.
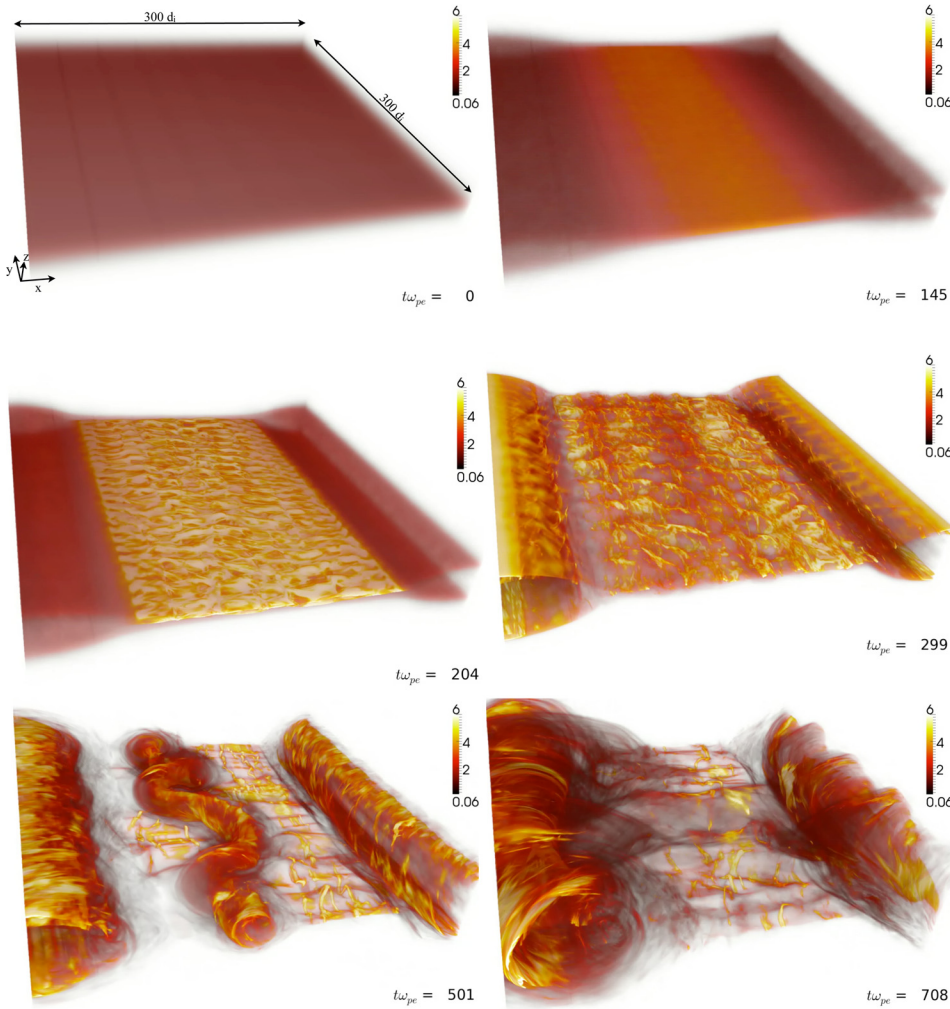
FIG. 2. Volume rendering of the current magnitude in the 3D simulations with $\sigma = 100$ at different times.

small scale ($\sim d_e$) kinked flux ropes are generated, and these quickly merge into large ropes. The scale of the small scale ropes is similar to that in the 2D simulations. The turbulence is fully developed to a power spectrum with a clear sign of inertial range that has an index "-2."[19]

Figure 3 shows the color-coded diagrams of (a) the bulk momentum in the x-direction $P_x = \Gamma v_x / c$, (b) the bulk momentum in the z-direction $P_z = \Gamma v_z / c$, and (c) the bulk Lorentz factor Γ. We find that the relativistic outflow can be generated in the reconnection layer. For higher σ, stronger bulk gamma can be found in the simulation.[19] It has been shown that the reconnection rate and inflow outflow speeds are similar for Harris and force-free current sheet.[75] The relativistic bulk motions may have a strong implication to the astrophysical high-energy radiation.[82–84]

Figure 4 shows the final energy spectra for $\sigma = 100$ with different initial temperatures $T_e = 3., 1.0, 0.3,$ and $0.1 m_e c^2$, respectively. While for high temperature case, the spectral index is close to $p = 2$; for lower initial temperatures, the energy spectra are harder and the spectral index approaches $p = 1$. This shows that as the ratio between the magnetic energy and the plasma energy increases, the spectral index becomes smaller.

Figure 5 shows the energy spectra for $\sigma = 10$ with different initial temperatures $T_e = 1.0, 0.3, 0.1, 0.03 m_e c^2$, respectively. While for high initial temperatures, the energization
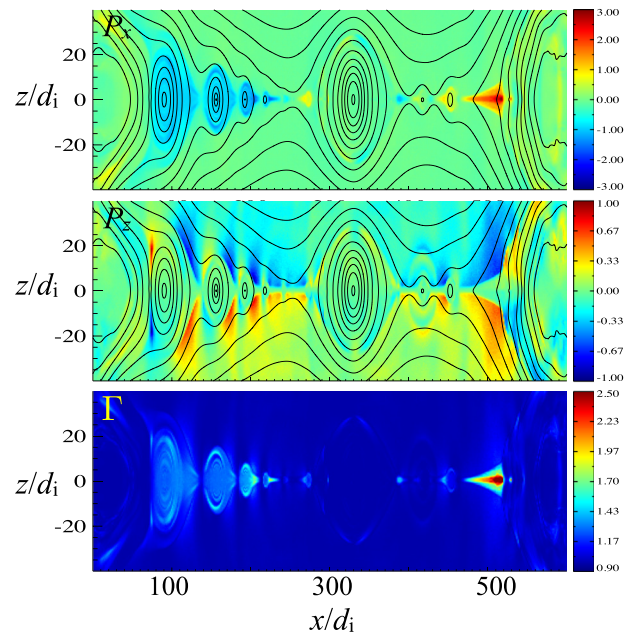

FIG. 3. Relativistic flows in the reconnection layer with $\sigma = 100$. Top panel: the bulk momentum in the x-direction $P_x = \Gamma v_x / c$. Middle panel: the bulk momentum in the z-direction $P_z = \Gamma v_z / c$. Bottom panel: the bulk Lorentz factor Γ.
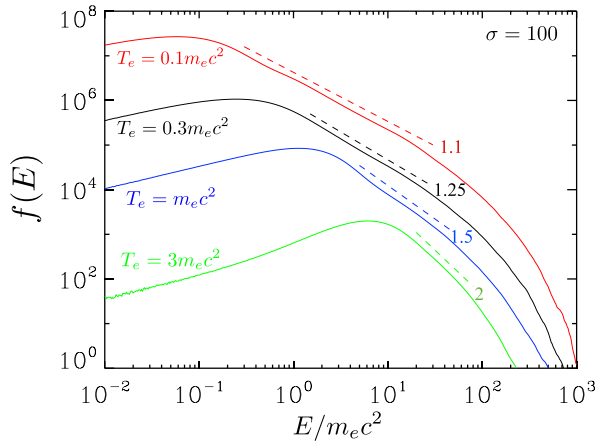
FIG. 4. Final energy spectra for cases with $\sigma = 100$ and different initial thermal temperatures $T_i = T_e = 3., 1.0, 0.3, 0.1 m_e c^2$.
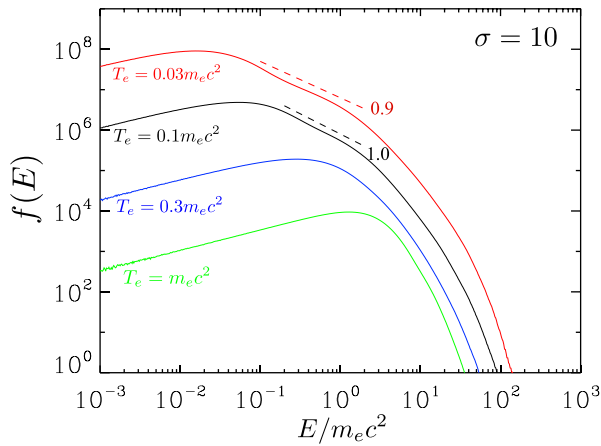

FIG. 5. Final energy spectra for cases with $\sigma = 10$ and different initial thermal temperatures $T_i = T_e = 1.0, 0.36, 0.1, 0.03 m_e c^2$.

is not significantly deviated from a thermal distribution, the cases with lower initial temperatures show a $p \sim 1$ energy spectrum. The result is similar for the case with $\sigma = 1$. Figure 6 shows the energy spectra for $\sigma = 1$ with different initial temperatures $T_e = 0.1, 0.03, 0.01, 0.003 m_e c^2$. While for high initial temperatures, the energization is not
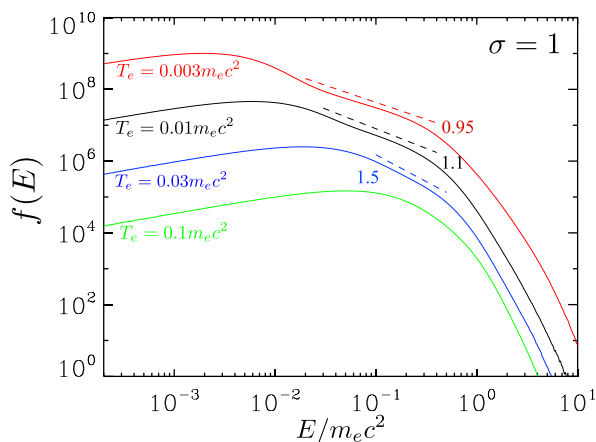

FIG. 6. Final energy spectra for cases with $\sigma = 1$ and different initial thermal temperatures $T_e = 0.1, 0.036, 0.01, 0.0036 m_e c^2$.

significantly deviated from a thermal distribution, the cases with lower initial temperatures show an overall $p \sim 1$ energy spectrum. Therefore, the generation of the nonthermal population of energetic particles appears to depend on the plasma β. As the plasma β decreases, the released magnetic energy exceeds the initial plasma energy, which leads to a nonthermal energization.

V. OUTSTANDING ISSUES AND CONCLUDING REMARK

The dissipation of magnetic field and particle energization in the magnetically dominated systems is of strong interest in high energy astrophysics. In this study, we have briefly reviewed recent progress and further studied the nonthermal particle acceleration. The primary new results of the paper are that the initial temperature plays a role in determining the spectral index of the nonthermal spectrum. While several earlier papers have concluded that the spectral index is smaller for higher σ, our simulations show that the spectral index approaches $p = 1$ for sufficiently low plasma β. While so far the results in general are consistent with our analytical prediction in the earlier papers,[18,19] it will be interesting to study the case with lower β when we are able to reduce the numerical noise that may cause artificial numerical heating. These new results need to be considered in interpreting the acceleration mechanisms from the PIC simulations. We also note that there are a number of other issues that cause uncertainties in the reconnection acceleration theory. Below, we outline several issues that need to be addressed in the future.

A. Dominant acceleration mechanism and power-law formation mechanism

It should be noted that although multiple papers have demonstrated efficient nonthermal energization and the formation of power-law distribution using PIC simulations, the dominant acceleration mechanism and the formation mechanism for the power-law distributions have not reached a consensus (see Section II for a discussion). Two main possibilities discussed in the literature are direct acceleration by the nonideal electric field in the diffusion region[16,65] and Fermi-like acceleration in the electric field induced by the motion of the reconnection driven flows.[18,19] Further efforts are required to distinguish the relative importance of the two (or other) mechanisms and their roles in the formation of power-law distribution, and determining the final spectral index.

B. Effect of 3D physics and MHD turbulence

Because of the level of computational cost, most of the kinetic studies of magnetic reconnection have been focusing on two-dimensional studies. There have been only a few 3D kinetic simulations of sufficient scale to allow a realistic interaction between various modes. For example, it has been shown that the oblique tearing modes and kink modes develop and interact each other, leading to a turbulent reconnection layer.[19,29,76,81] However, those simulations have found about the same reconnection rate compared to 2D

studies, indicating the 3D effects do not significantly alter the reconnection rate, although what determines the reconnection rate found in kinetic simulations is still a controversial topic. While early simulations show that kink instability may prohibit the nonthermal acceleration,[85] recent large scale simulations have shown that nonthermal acceleration can still develop despite the growth of the kink instability.[16,18,19] It will be interesting to analyze the effects of 3D physics to different acceleration mechanisms for the nonthermal acceleration.

A closely related topic is the influence of turbulence on reconnection. The effects of MHD turbulence on the reconnection physics and the acceleration of particles have not been fully understood. Several numerical studies have shown that magnetic turbulence can develop from a three-dimensional reconnection layer, but the evidence that the turbulence has strong effect on reconnection physics is still missing. It will also be interesting to study if the self-excited or externally driven turbulence will significantly change the mechanism for nonthermal particle acceleration.

C. Effects that lead to a steeper spectrum

In agreement with other recent papers,[16,18,19,46–49] this work shows that the spectral index in simulation is often much harder than commonly observed in space and inferred from astrophysical emissions. Although there is some observational evidence in support of the hard spectrum [e.g., Ref. 86], the power-law index predicted by the PIC simulation is systematically harder than most observations. More seriously, for a power-law spectrum with spectral index $p < 2$, the total energy contained in the distribution quickly increases with particle energy. This limits the maximum energy in the power-law predicted from the available magnetic energy. We have analytically shown that allowing particle escape from the reconnection region will produce a steeper spectrum.[18,19] However, most of the kinetic simulations so far have used periodic boundary conditions. Nevertheless, these recent results suggest that it is important to consider the effects that can lead to a softer spectrum such as open boundary simulations in the future.

ACKNOWLEDGMENTS

[1]D. Biskamp, *Magnetic Reconnection in Plasmas* (Cambridge University Press, 2000).

[2]E. Priest and T. Forbes, *Magnetic Reconnection* (Cambridge University Press, Cambridge, UK, 2000).

[3]M. Yamada, R. Kulsrud, and H. Ji, Rev. Mod. Phys. **82**, 603 (2010).

[4]E. G. Zweibel and M. Yamada, ARA&A **47**, 291 (2009).

[5]M. Øieroset, R. P. Lin, T. D. Phan, D. E. Larson, and S. D. Bale, Phys. Rev. Lett. **89**, 195001 (2002).

[6]S. Masuda, T. Kosugi, H. Hara, S. Tsuneta, and Y. Ogawara, Nature **371**, 495 (1994).

[7]S. Krucker, H. S. Hudson, L. Glesener, S. M. White, S. Masuda, J.-P. Wuelser, and R. P. Lin, Astrophys. J. **714**, 1108 (2010).

[8]J. Ambrosiano, W. H. Matthaeus, M. L. Goldstein, and D. Plante, J. Geophys. Res. **93**, 14383, doi:10.1029/JA093iA12p14383 (1988).

[9]M. Hoshino, T. Mukai, T. Terasawa, and I. Shinohara, J. Geophys. Res. **106**, 25979, doi:10.1029/2001JA900052 (2001).

[10]E. M. de Gouveia dal Pino and A. Lazarian, Astron. Astrophys. **441**, 845 (2005).

[11]J. F. Drake, M. Swisdak, H. Che, and M. A. Shay, Nature **443**, 553 (2006).

[12]X. R. Fu, Q. M. Lu, and S. Wang, Phys. Plasmas **13**, 012309 (2006).

[13]P. L. Pritchett, J. Geophys. Res.: Space Phys. **111**, 10212, doi:10.1029/2006JA011793 (2006).

[14]M. Oka, T.-D. Phan, S. Krucker, M. Fujimoto, and I. Shinohara, Astrophys. J. **714**, 915 (2010).

[15]L. O. Drury, MNRAS **422**, 2474 (2012).

[16]L. Sironi and A. Spitkovsky, Astrophys. J. **783**, L21 (2014).

[17]J. T. Dahlin, J. F. Drake, and M. Swisdak, Phys. Plasmas **21**, 092304 (2014).

[18]F. Guo, H. Li, W. Daughton, and Y.-H. Liu, Phys. Rev. Lett. **113**, 155005 (2014).

[19]F. Guo, Y.-H. Liu, W. Daughton, and H. Li, Astrophys. J. **806**, 167 (2015).

[20]G. P. Zank, J. A. le Roux, G. M. Webb, A. Dosch, and O. Khabarova, Astrophys. J. **797**, 28 (2014).

[21]J. A. le Roux, G. P. Zank, G. M. Webb, and O. Khabarova, Astrophys. J. **801**, 112 (2015).

[22]N. F. Loureiro, A. A. Schekochihin, and S. C. Cowley, Phys. Plasmas **14**, 100703 (2007).

[23]W. Daughton, V. Roytershteyn, B. J. Albright, H. Karimabadi, L. Yin, and K. J. Bowers, Phys. Rev. Lett. **103**, 065004 (2009).

[24]A. Bhattacharjee, Y.-M. Huang, H. Yang, and B. Rogers, Phys. Plasmas **16**, 112102 (2009).

[25]D. A. Uzdensky, N. F. Loureiro, and A. A. Schekochihin, Phys. Rev. Lett. **105**, 235002 (2010).

[26]A. Lazarian and E. T. Vishniac, Astrophys. J. **517**, 700 (1999).

[27]G. Kowal, A. Lazarian, E. T. Vishniac, and K. Otmianowska-Mazur, Astrophys. J. **700**, 63 (2009).

[28]N. F. Loureiro, D. A. Uzdensky, A. A. Schekochihin, S. C. Cowley, and T. A. Yousef, MNRAS **399**, L146 (2009).

[29]W. Daughton, V. Roytershteyn, H. Karimabadi, L. Yin, B. J. Albright, B. Bergen, and K. J. Bowers, Nat. Phys. **7**, 539 (2011).

[30]W. Daughton, Nakamura, T. K. M., H. Karimabadi, V. Roytershteyn, and B. Loring, Phys. Plasmas **21**, 052307 (2014).

[31]Y.-M. Huang and A. Bhattacharjee, Astrophys. J. **818**, 20 (2016).

[32]C. Huang, Q. Lu, F. Guo, M. Wu, A. Du, and S. Wang, Geophys. Res. Lett. **42**, 7282, doi:10.1002/2015GL065690 (2015).

[33]C. Thompson, MNRAS **270**, 480 (1994).

[34]G. Drenkhahn and H. C. Spruit, Astron. Astrophys. **391**, 1141 (2002).

[35]A. A. Abdo, M. Ackermann, M. Ajello, A. Allafort, L. Baldini, J. Ballet, G. Barbiellini, D. Bastieri, K. Bechtol, R. Bellazzini, B. Berenji, R. D. Blandford, E. D. Bloom, E. Bonamente, A. W. Borgland, A. Bouvier, T. J. Brandt, J. Bregeon, A. Brez, M. Brigida, P. Bruel, R. Buehler, S. Buson, G. A. Caliandro, R. A. Cameron, A. Cannon, P. A. Caraveo, J. M. Casandjian, Elik, E. Charles, A. Chekhtman, C. C. Cheung, J. Chiang, S. Ciprini, R. Claus, J. Cohen-Tanugi, L. Costamante, S. Cutini, F. D'Ammando, C. D. Dermer, A. de Angelis, A. de Luca, F. de Palma, S. W. Digel, E. do Couto e Silva, P. S. Drell, A. Drlica-Wagner, R. Dubois, D. Dumora, C. Favuzzi, S. J. Fegan, E. C. Ferrara, W. B. Focke, P. Fortin, M. Frailis, Y. Fukazawa, S. Funk, P. Fusco, F. Gargano, D. Gasparrini, N. Gehrels, S. Germani, N. Giglietto, F. Giordano, M. Giroletti, T. Glanzman, G. Godfrey, I. A. Grenier, M.-H. Grondin, J. E. Grove, S. Guiriec, D. Hadasch, Y. Hanabata, A. K. Harding, K. Hayashi, M. Hayashida, E. Hays, D. Horan, R. Itoh, G. Jhannesson, A. S. Johnson, T. J. Johnson, D. Khangulyan, T. Kamae, H. Katagiri, J. Kataoka, M. Kerr, J. Kndlseder, M. Kuss, J. Lande, L. Latronico, S.-H. Lee, M. Lemoine-Goumard, F. Longo, F. Loparco, P. Lubrano, G. M. Madejski, A. Makeev, M. Marelli, M. N. Mazziotta, J. E. McEnery, P. F. Michelson, W. Mitthumsiri, T. Mizuno, A. A. Moiseev, C. Monte, M. E. Monzani, A. Morselli, I. V. Moskalenko, S. Murgia, T. Nakamori, M. Naumann-Godo, P. L. Nolan, J. P. Norris, E. Nuss, T. Ohsugi, A. Okumura, N. Omodei, J. F. Ormes, M. Ozaki, D. Paneque, D. Parent, V. Pelassa, M. Pepe, M. Pesce-Rollins, M.

Pierbattista, F. Piron, T. A. Porter, S. Rain, R. Rando, P. S. Ray, M. Razzano, A. Reimer, O. Reimer, T. Reposeur, S. Ritz, R. W. Romani, H. F.-W. Sadrozinski, D. Sanchez, Parkinson, P. M. Saz, J. D. Scargle, T. L. Schalk, C. Sgr, E. J. Siskind, P. D. Smith, G. Spandre, P. Spinelli, M. S. Strickman, D. J. Suson, H. Takahashi, T. Takahashi, T. Tanaka, J. B. Thayer, D. J. Thompson, L. Tibaldo, D. F. Torres, G. Tosti, A. Tramacere, E. Troja, Y. Uchiyama, J. Vandenbroucke, V. Vasileiou, G. Vianello, V. Vitale, P. Wang, K. S. Wood, Z. Yang, and M. Ziegler, Science **331**, 739 (2011).

[36]M. Tavani, A. Bulgarelli, V. Vittorini, A. Pellizzoni, E. Striani, P. Caraveo, M. C. Weisskopf, A. Tennant, G. Pucella, A. Trois, E. Costa, Y. Evangelista, C. Pittori, F. Verrecchia, Del E. Monte, R. Campana, M. Pilia, De A. Luca, I. Donnarumma, D. Horns, C. Ferrigno, C. O. Heinke, M. Trifoglio, F. Gianotti, S. Vercellone, A. Argan, G. Barbiellini, P. W. Cattaneo, A. W. Chen, T. Contessi, F. D'Ammando, G. DeParis, G. Di Cocco, G. Di Persio, M. Feroci, A. Ferrari, M. Galli, A. Giuliani, M. Giusti, C. Labanti, I. Lapshov, F. Lazzarotto, P. Lipari, F. Longo, F. Fuschino, M. Marisaldi, S. Mereghetti, E. Morelli, E. Moretti, A. Morselli, L. Pacciani, F. Perotti, G. Piano, P. Picozza, M. Prest, M. Rapisarda, A. Rappoldi, A. Rubini, S. Sabatini, P. Soffitta, E. Vallazza, A. Zambra, D. Zanello, F. Lucarelli, P. Santolamazza, P. Giommi, L. Salotti, and G. F. Bignami, Science **331**, 736 (2011).

[37]B. Zhang and H. Yan, Astrophys. J. **726**, 90 (2011).

[38]D. A. Uzdensky, Space Sci. Rev. **160**, 45 (2011).

[39]J. C. McKinney and D. A. Uzdensky, MNRAS **419**, 573 (2012).

[40]J. Arons, Space Sci. Rev. **173**, 341 (2012).

[41]C. Yu and L. Huang, Astrophys. J. **771**, L46 (2013).

[42]H. Zhang, X. Chen, M. Böttcher, F. Guo, and H. Li, Astrophys. J. **804**, 58 (2015).

[43]A. Celotti and G. Ghisellini, MNRAS **385**, 283 (2008).

[44]S. Tsuneta, S. Masuda, T. Kosugi, and J. Sato, Astrophys. J. **478**, 787 (1997).

[45]A. A. Galeev, R. Rosner, and G. S. Vaiana, Astrophys. J. **229**, 318 (1979).

[46]M. Melzani, R. Walder, D. Folini, C. Winisdoerffer, and J. M. Favre, Astron. Astrophys. **570**, A112 (2014).

[47]X. Li, F. Guo, H. Li, and G. Li, Astrophys. J. **811**, L24 (2015).

[48]G. R. Werner, D. A. Uzdensky, B. Cerutti, K. Nalewajko, and M. C. Begelman, Astrophys. J. **816**, L8 (2016).

[49]F. Guo, X. Li, H. Li, W. Daughton, B. Zhang, N. Lloyd-Ronning, Y.-H. Liu, H. Zhang, and W. Deng, Astrophys. J. **818**, L9 (2016).

[50]T. W. Speiser, J. Geophys. Res. **70**, 4219, doi:10.1029/JZ070i017p04219 (1965).

[51]C. Huang, Q. Lu, and S. Wang, Phys. Plasmas **17**, 072306 (2010).

[52]J. Egedal, W. Daughton, and A. Le, Nat. Phys. **8**, 321 (2012).

[53]R. Wang, Q. Lu, Y. V. Khotyaintsev *et al.*, Geophys. Res. Lett. **41**, 4851, doi:10.1002/2014GL061157 (2014).

[54]J. Egedal, W. Daughton, A. Le, and A. L. Borg, Phys. Plasmas **22**, 101208 (2015).

[55]M. Wu, C. Huang, Q. Lu, M. Volwerk, R. Nakamura, Z. Vrs, T. Zhang, and S. Wang, J. Geophys. Res.: Space Phys. **120**, 6320 (2015).

[56]S. Y. Huang *et al.*, Geophys. Res. Lett. **39**, 11103, doi:10.1029/2012GL051946 (2012).

[57]R. Wang, Q. Lu, A. Du, and S. Wang, Phys. Rev. Lett. **104**, 175003 (2010).

[58]R. Wang, Q. Lu, X. Li, C. Huang, and S. Wang, J. Geophys. Res.: Space Phys. **115**, A11201, doi:10.1029/2010JA015473 (2010).

[59]C. Huang, M. Wu, Q. Lu, R. Wang, and S. Wang, J. Geophys. Res.: Space Phys. **120**, 1759 (2015).

[60]H. S. Fu, Y. V. Khotyaintsev, André, M., and A. Vaivads, Geophys. Res. Lett. **38**, 16104, doi:10.1029/2011GL048528 (2011).

[61]H. S. Fu, Y. V. Khotyaintsev, A. Vaivads, A. Retinò, and M. André, Nat. Phys. **9**, 426 (2013).

[62]M. Wu, Q. Lu, M. Volwerk *et al.*, J. Geophys. Res.: Space Phys. **118**, 4804 (2013).

[63]S. Zenitani and M. Hoshino, Astrophys. J. **562**, L63 (2001).

[64]S. Zenitani and M. Hoshino, Astrophys. J. **670**, 702 (2007).

[65]N. Bessho and A. Bhattacharjee, Astrophys. J. **750**, 129 (2012).

[66]B. Cerutti, G. R. Werner, D. A. Uzdensky, and M. C. Begelman, Astrophys. J. **770**, 147 (2013).

[67]A. Spitkovsky and L. Sironi, private communication on the formation of power laws and dominant acceleration mechanism in relativistic magnetic reconnection (2015).

[68]K. Nalewajko, D. A. Uzdensky, B. Cerutti, G. R. Werner, and M. C. Begelman, Astrophys. J. **815**, 101 (2015).

[69]F. V. Coroniti, Astrophys. J. **349**, 538 (1990).

[70]V. S. Titov, K. Galsgaard, and T. Neukirch, Astrophys. J. **582**, 1172 (2003).

[71]M. Wan, A. F. Rappazzo, W. H. Matthaeus, S. Servidio, and S. Oughton, Astrophys. J. **797**, 63 (2014).

[72]V. Zhdankin, S. Boldyrev, J. Mason, and J. C. Perez, Phys. Rev. Lett. **108**, 175004 (2012).

[73]K. D. Makwana, V. Zhdankin, H. Li, W. Daughton, and F. Cattaneo, Phys. Plasmas **22**, 042902 (2015).

[74]H. Che, J. F. Drake, and M. Swisdak, Nature **474**, 184 (2011).

[75]Y.-H. Liu, F. Guo, W. Daughton, H. Li, and M. Hesse, Phys. Rev. Lett. **114**, 095002 (2015).

[76]Y.-H. Liu, W. Daughton, H. Karimabadi, H. Li, and V. Roytershteyn, Phys. Rev. Lett. **110**, 265004 (2013).

[77]J. G. Kirk and O. Skjæraasen, Astrophys. J. **591**, 366 (2003).

[78]K. J. Bowers, B. J. Albright, L. Yin, W. Daughton, V. Roytershteyn, B. Bergen, and T. J. T. Kwan, J. Phys. Conf. Ser. **180**, 012055 (2009).

[79]J. Birn *et al.*, J. Geophys. Res. **106**, 3715, doi:10.1029/1999JA900449 (2001).

[80]W. Daughton and H. Karimabadi, Phys. Plasmas **14**, 072303 (2007).

[81]L. Yin, W. Daughton, H. Karimabadi, B. J. Albright, K. J. Bowers, and J. Margulies, Phys. Rev. Lett. **101**, 125001 (2008).

[82]W. Deng, H. Li, B. Zhang, and S. Li, Astrophys. J. **805**, 163 (2015).

[83]D. Giannios, D. A. Uzdensky, and M. C. Begelman, MNRAS **395**, L29 (2009).

[84]D. Kagan, E. Nakar, and T. Piran, e-print arXiv:1601.07349.

[85]S. Zenitani and M. Hoshino, Astrophys. J. **677**, 530 (2008).

[86]M. Hayashida, K. Nalewajko, G. M. Madejski, M. Sikora, R. Itoh, M. Ajello, R. D. Blandford, S. Buson, J. Chiang, Y. Fukazawa, A. K. Furniss, C. M. Urry, I. Hasan, F. A. Harrison, D. M. Alexander, M. Balokovi, D. Barret, S. E. Boggs, F. E. Christensen, W. W. Craig, K. Forster, P. Giommi, B. Grefenstette, C. Hailey, A. Hornstrup, T. Kitaguchi, J. E. Koglin, K. K. Madsen, P. H. Mao, H. Miyasaka, K. Mori, M. Perri, M. J. Pivovaroff, S. Puccetti, V. Rana, D. Stern, G. Tagliaferri, N. J. Westergaard, W. W. Zhang, A. Zoglauer, M. A. Gurwell, M. Uemura, H. Akitaya, K. S. Kawabata, K. Kawaguchi, Y. Kanda, Y. Moritani, K. Takaki, T. Ui, M. Yoshida, A. Agarwal, and A. C. Gupta, Astrophys. J. **807**, 79 (2015).